Docosahexaenoic Acid Enhances Segregation of Lipids between Raft and Nonraft Domains: ^{2}H-NMR Study

Smita P. Soni,* Daniel S. LoCascio,† Yidong Liu,‡ Justin A. Williams,* Robert Bittman,‡ William Stillwell,† and Stephen R. Wassall*

*Department of Physics, Indiana University–Purdue University Indianapolis, Indianapolis, Indiana 46202-3273; †Department of Biology, Indiana University–Purdue University Indianapolis, Indianapolis, Indiana 46202-5132; and ‡Department of Chemistry and Biochemistry, Queens College of CUNY, Flushing, New York 11367-1597

ABSTRACT Solid-state ^{2}H-NMR of [$^2H_{31}$]-*N*-palmitoylsphingomyelin ([$^2H_{31}$]16:0SM, PSM*), supplemented by differential scanning calorimetry, was used for the first time, to our knowledge, to investigate the molecular organization of the sphingolipid in 1:1:1 mol mixtures with 1-palmitoyl-2-oleoyl-*sn*-glycero-3-phosphoethanolamine (16:0–18:1PE, POPE) or 1-palmitoyl-2-docosahexaenoyl-*sn*-glycero-3-phosphoethanolamine (16:0–22:6PE, PDPE) and cholesterol. When compared with ^{2}H-NMR data for analogous mixtures of [$^2H_{31}$]16:0–18:1PE (POPE*) or [$^2H_{31}$]16:0-22:6PE (PDPE*) with egg SM and cholesterol, molecular interactions of oleic acid (OA) versus docosahexaenoic acid (DHA) are distinguished, and details of membrane architecture emerge. SM-rich, characterized by higher-order, and PE-rich, characterized by lower-order, domains $<$20 nm in size are formed in the absence and presence of cholesterol in both OA- and DHA-containing membranes. Although acyl chain order within both domains increases on the addition of sterol to the two systems, the resultant differential in order between SM- and PE-rich domains is almost a factor of 3 greater with DHA than with OA. Our interpretation is that the aversion that cholesterol has for DHA—but not for OA—excludes the sterol from DHA-containing, PE-rich (nonraft) domains and excludes DHA from SM-rich/cholesterol-rich (raft) domains. We attribute, in part, the diverse health benefits associated with dietary consumption of DHA to an alteration in membrane domains.

INTRODUCTION

The disease-countering benefits and necessity for neurologic function of the ω-3 family of polyunsaturated fatty acids (PUFA) are well documented (1,2). Docosahexaenoic acid (DHA, 22:6$^{\Delta 4,7,10,13,16,19}$), which is the longest (22 carbons) and most unsaturated (6 double bonds) member of this family found naturally, is particularly influential (3). The numerous varieties of human affliction that it alleviates include heart disease, cancer, rheumatoid arthritis, asthma, lupus, and schizophrenia (3–5). To participate in so many seemingly unrelated processes, DHA must function at a fundamental level that is common to most cells. We (3–5), and others (6,7), have proposed that the plasma membrane is a major site of action. According to our model, low affinity of DHA for cholesterol accentuates the formation of liquid-disordered regions enriched in DHA-containing phospholipids and liquid-ordered lipid rafts enriched in sphingomyelin (SM) and cholesterol. Introduction of DHA from the diet enhances the lateral segregation of these two distinct types of domains and the accompanying changes in location of signaling proteins, for which rafts serve as the platform, then modulate cellular events.

Initially, biological membranes were envisaged in the fluid mosaic model as a phospholipid bilayer matrix within which lipids and proteins were mixed homogeneously (8). A refinement of this picture has evolved during the last decade, whereby the biological membranes contain functional domains characterized by different composition and spatial arrangement of the membrane-constituting lipids (9–11). These domains are the result of unequal affinities between lipids species or between lipids and membrane proteins. A lipid domain that has received a great deal of attention is the lipid raft, liquid-ordered regions 10–200 nm in size and enriched in cholesterol and sphingolipids that float in a ''sea'' of liquid-disordered phospholipids (10–13). When clustered together, they serve as a site for the function of essential cell-signaling proteins such as glycosylinositol phospholipid (GPI)-linked proteins in the outer leaflet of the plasma membrane (14). Raft formation is attributed to the saturated nature of sphingolipid acyl chains (15). Their predominantly all-*trans* extended conformation packs well with the rigid steroid moiety of cholesterol; raft stability is conferred further by hydrogen bonding of the sphingosine backbone amide to the hydroxyl group of an adjacent sphingolipid, as well as to the hydroxyl group of the sterol (16). Phospholipids containing DHA, in contrast, represent the opposite extreme to sphingolipids in affinity for cholesterol. Close proximity to the steroid moiety is deterred by the wide variety of rapidly varying conformers that are adopted because polyunsaturated chains are tremendously disordered, and affinity for the sterol is low (4). We hypothesize that, when DHA-containing phospholipids are introduced into mixed membranes that include the lipid raft molecules SM and cholesterol, they enhance the segregation of cholesterol into SM-rich/sterol-rich rafts and

Submitted October 9, 2007, and accepted for publication February 25, 2008.

Address reprint requests to Stephen R. Wassall, Tel.: 317-274-6908; Fax: 317-274-2393; E-mail: swassall@iupui.edu.

Editor: Thomas J. McIntosh.

0006-3495/08/07/203/12 $2.00

doi: 10.1529/biophysj.107.123612

away from DHA-rich domains that exclude the sterol (3–5). A modulation of cellular events is produced by movement of signaling proteins in and/or out of rafts due to changes in plasma membrane architecture that occur after phospholipids incorporate the DHA that comes from diet. This modulation, in part, is the origin to which we attribute the myriad of health benefits associated with consumption of the PUFA.

Evidence in support of our hypothesis has been garnered by applying a range of biophysical methodologies to a membrane model that we have developed comprised of 1-palmitoyl-2-docosahexaenoyl-*sn*-glycero-3-phosphoethanolamne (16:0-22:6PE, PDPE) in mixtures with SM and cholesterol (17). PE, which is the second-most abundant phospholipid in mammalian plasma membranes after phosphatidylcholine (PC) (18), was selected; it is preferred over PC for the uptake of DHA that occurs at the *sn*-2 position while a saturated chain occupies the *sn*-1 position (19,20). PE also possesses a reduced affinity for cholesterol relative to PC and SM that is exemplified by the smaller solubility measured for the sterol in DHA-containing PE versus PC (21). Differential scanning calorimetry (DSC), detergent extraction, and solid-state ^{2}H-NMR spectroscopy are among the principal techniques that we have applied to PE/SM and PE/SM/cholesterol mixtures in a series of studies (17,22). Detergent extraction of PDPE/egg SM/cholesterol (1:1:1 mol) membranes showed that egg SM and cholesterol phase separate almost exclusively (>90%) into a detergent-resistant membrane (DRM) fraction (the biochemical hallmark of lipid rafts (11)), whereas PDPE predominantly phase separates (70%) into a nonraft detergent-soluble membrane (DSM) fraction (17). In contrast, much less phase separation (22%) into DSM was observed for 1-palmitoyl-2-oleoyl-*sn*-glycero-3-phosphoethanolamine (16:0–18:1PE, POPE) in POPE/egg SM/cholesterol (1:1:1 mol) in which polyunsaturated DHA was replaced by more ''typical'' monounsaturated oleic acid (OA) (18) at the *sn*-2 position of PE. As in the DHA-containing system, egg SM and cholesterol were found almost entirely (>90%) in DRM in the control OA-containing system. Solid-state ^{2}H-NMR spectra comparing the effect of cholesterol on [$^2H_{31}$]16:0–22:6PE (PDPE*)/egg SM (1:1:1 mol) and [$^2H_{31}$]16:0–18:1PE (POPE*)/egg SM (1:1:1 mol) demonstrated a diminished interaction between the sterol and DHA-relative to OA-containing PE (17). The increase in the average order parameter $\bar{S}_{CD}$ of the perdeuterated [$^2H_{31}$]16:0 *sn*-1 chain for the polyunsaturated component ($\Delta\bar{S}_{CD} = 0.039$) in the mixed membrane was more than a factor of 2 less than for the monounsaturated component ($\Delta\bar{S}_{CD} = 0.100$) following the addition of cholesterol at 40°C.

In this study, we switch the focus from PE to SM in our model system. Solid-state ^{2}H-NMR, complemented by DSC, is used to compare [$^2H_{31}$]-*N*-palmitoylsphingomyelin ([$^2H_{31}$]16:0SM, PSM*) in PDPE/PSM* (1:1 mol) with POPE/PSM* (1:1 mol) in the absence and presence of cholesterol (1:1:1 mol). PSM is the major constituent (~85%) of egg SM (23). Thus, the results obtained provide information about the impact of the sterol on the molecular organization of the SM component in mixed membranes that closely approximate those membranes for which the PE component was observed previously. We examine whether our hypothesis–the aversion of cholesterol for DHA promotes the formation of PUFA-rich/sterol-poor domains, as implied by the spectra recorded for PDPE* versus POPE* in PE/egg SM/cholesterol (1:1:1 mol) mixtures (17)—is corroborated by the spectra observed for PSM* in the corresponding PE/PSM/cholesterol (1:1:1 mol) mixtures.

MATERIALS AND METHODS

Materials

POPE, PDPE, and egg SM were purchased from Avanti Polar Lipids (Alabaster, AL). Cholesterol and deuterium depleted water were obtained from Sigma Chemical (St. Louis, MO). Cambridge Isotope Laboratories (Andover, MA) was the source of [$^2H_{31}$]palmitic acid. Lipid purity was confirmed by thin-layer chromatography.

PSM* synthesis

PSM* was synthesized by *N*-acylation of *D*-erythro-sphingosylphosphocholine with the *p*-nitrophenyl ester of [$^2H_{31}$]palmitic acid in dichloromethane/*N*,*N*-dimethylformamide (2:5 vol/vol) at room temperature under nitrogen (24). The volatiles were removed under vacuum, and the product was purified by column chromatography (elution with chloroform/methanol/water 65:35:5 v/v) followed by filtration through a Cameo filter (Fisher Scientific, Pittsburgh, PA) to remove suspended silica gel and lyophilization.

PSM isolation

PSM was isolated from egg SM by reverse-phase high-performance liquid chromatography (HPLC) (25). In brief, egg SM was run through a dual-pump HPLC setup (Beckman Coulter, Fullerton, CA) using an analytical reverse-phase column (5-μm particle size, 250 mm × 10 mm) (Alltima C-18 RP; Alltech Associates, Deerfield, IL) and methanol with 6 vol % water as the eluent (4.2 mL/min at 40°C). Purity of the PSM obtained was verified by ^{1}H-NMR spectroscopy and mass spectrometry.

^{2}H-NMR sample preparation

Lipid mixtures (75–90 mg total lipid) comprised of POPE/PSM* (1:1 mol), POPE/PSM*/cholesterol (1:1:1 mol), PDPE/PSM* (1:1 mol), and PDPE/PSM*/cholesterol (1:1:1 mol) were codissolved in chloroform. The organic solvent was evaporated under a gentle stream of argon followed by vacuum pumping to ensure removal of solvent traces. Each lipid mixture was hydrated to 50 wt % with 50 mM Tris buffer (pH 7.5) and vortexed vigorously. Deuterium depleted water (~2 mL) was added to allow measurement of pH, which was adjusted to 7.5. Three lyophilizations in the presence of excess deuterium depleted water were then performed to remove naturally abundant ^{2}HHO. After finally hydrating to 50 wt %, the resultant samples were transferred to a 5-mm NMR tube that was sealed with a Teflon-coated plug. They were stored at −80°C and equilibrated at room temperature before the experiments. Precautions to prevent oxidation were taken throughout sample preparation. All manipulations were performed in an argon atmosphere within a homebuilt glovebox; buffer and deuterium depleted water were degassed thoroughly, and exposure to light was minimized (22).

^{2}H-NMR spectroscopy

Solid-state ^{2}H-NMR experiments were performed on a homebuilt spectrometer operating at 27.6 MHz with a super-conducting magnet (Nalorac Cryogenics, Martinez, CA) operating at 4.2 T (26). A computer (Compaq, Houston, TX) controlled the spectrometer. Pulse programming was accomplished with an in-house assembled programmable pulse generator, while signals were acquired in quadrature using a digital oscilloscope (R1200 M dual channel; Rapid Systems, Seattle, WA). Sample temperature was regulated to ±0.5°C by a temperature controller (1600 Series; Love Controls, Michigan City, IN). A phase-alternated quadrupolar echo sequence $(90^\circ_x - t - 90^\circ_y - \text{acquire} - \text{delay})_n$ that eliminates spectral distortion due to receiver recovery time was implemented to collect spectra (27). Unless otherwise stated, spectral parameters were 90° pulse-width ≈6 μs; separation between pulses $t = 50$ μs; delay between pulse sequences = 1.0 s (gel phase) or 1.5 s (liquid crystalline phase); sweep width = ±250 kHz (gel phase) or ±100 kHz (liquid crystalline phase); dataset = 2 K; and number of transients = 2048.

Analysis of ^{2}H-NMR spectra

First moments M_1 were calculated from ^{2}H-NMR spectra for PSM* in POPE/PSM* (1:1 mol), POPE/PSM*/cholesterol (1:1:1 mol), PDPE/PSM* (1:1:1 mol), and PDPE/PSM*/cholesterol (1:1:1 mol) mixtures with the following:

$$M_1 = \frac{\int_{-\infty}^{\infty} |\omega| f(\omega) d\omega}{\int_{-\infty}^{\infty} f(\omega) d\omega}, \quad (1)$$

where ω is the frequency with respect to the central Larmor frequency ω_0 and $f(\omega)$ is the lineshape (28). In practice the integral was a summation over the digitized data. The expression in the following:

$$M_1 = \frac{\pi}{\sqrt{3}} \left(\frac{e^2 qQ}{h} \right) |\overline{S}_{CD}| \quad (2)$$

relates M_1 to the $\overline{S}_{CD}$ of the perdeuterated palmitoyl amide side chain via the static quadrupole coupling constant $(e^2qQ/h) = 167$ kHz in the lamellar liquid crystalline phase.

Spectra were also fast Fourier transform depaked to enhance resolution in the lamellar liquid crystalline phase (26). This numerical procedure extracts a spectrum from the powder pattern signal that is representative of a planar membrane of single alignment. The depaked spectra consist of doublets with quadrupolar splittings $\Delta\nu(\theta)$ that equate to order parameters by the following:

$$\Delta\nu(\theta) = \frac{3}{2} \left(\frac{e^2 qQ}{h} \right) |S_{CD}| P_2(\cos\theta), \quad (3)$$

where $\theta = 0°$ is the angle the membrane normal makes with the magnetic field and $P_2(\cos\theta)$ is the second-order Legendre polynomial. Smoothed profiles of order along the perdeuterated palmitoyl amide side chain then were constructed on the basis of integrated intensity assuming monotonic variation toward the disordered center of the bilayer (29). Constraints imposed on the initial orientation of the chain render the C2 position an exception to this assumption, and S_{CD} values there were assigned on the basis of intensity and comparison with previous work on selectively deuterated analogs of PSM (30).

DSC

DSC experiments were conducted as described previously (31). The preparation of aqueous dispersions of 0.5 wt % POPE/PSM (1:1 mol), POPE/PSM/cholesterol (1:1:1 mol), PDPE/PSM (1:1 mol), and PDPE/PSM/cholesterol (1:1:1 mol) in 10 mM phosphate buffer (pH 7.4) was similar to that used to prepare the NMR samples, except that lyophilization to remove natural abundance ^{2}HHO was unnecessary. Degassing in particular was critical because dissolved gases have the potential to attack PUFA and contribute noise to high-sensitivity calorimetry measurements. Heating and cooling scans for 500-μL samples were run at 0.125°C/min from −10°C to 60°C against a lipid-free control buffer on a multicell differential scanning calorimeter (Calorimetry Sciences, Lindin, UT). Only the cooling scans are presented, although data derived from both scans appeared nearly identical. Baseline subtraction was performed with CpCalc version 2.1 (Applied Thermodynamics, Longwood, FL) software, and analysis of endotherms was carried out using graphing software (Origin 7.0; OriginLab, Northampton, MA).

RESULTS

Phase behavior

^{2}H-NMR

Solid-state ^{2}H-NMR spectra for 50 wt % aqueous dispersions of POPE/PSM* (1:1 mol), PDPE/PSM* (1:1 mol), POPE/PSM*/cholesterol (1:1:1 mol), and PDPE/PSM*/cholesterol (1:1:1 mol) in 50 mM Tris (pH 7.5) were obtained as a function of temperature to study the phase behavior of the perdeuterated sphingolipid in lipid mixtures with OA- and DHA-containing PE in the absence and presence of cholesterol. The spectra were collected from −30°C to 50°C. This range of temperature encompasses the gel to liquid crystalline transition for single component membranes of PSM at 41°C (32), POPE at 25.5°C (22), and PDPE at 2.2°C (22). Only one study of PSM* has been published to date, which used membranes aligned between glass slides to improve spectral resolution (30). We use multilamellar dispersions and apply lineshape analysis to observed powder patterns that are comprised of a superposition of signals from the random orientational distribution of membranes that exists within a sample.

Representative examples of the spectra for POPE/PSM* (1:1 mol) are shown in Fig. 1 (*left panel*). They display changes in the spectral shape that accompany the transition between gel and liquid crystalline states as the suspension is heated. The wide, relatively featureless spectrum with edges at ±63 kHz that was recorded at −23°C is typical of a lamellar gel phase (Fig. 1 *a*). The [$^2H_{31}$]16:0 chains of PSM* are rigid, and their slow rotational diffusion confers nonaxial symmetry on the spectral shape (17). On raising the temperature, additional molecular motions are introduced that result in spectral narrowing. Inspection of the spectrum at 12°C reveals that, although still broad and gel-like, there is less intensity in the wings (Fig. 1 *b*). At higher temperature, shoulders around ±20 kHz appear superposed on the broad gel component and grow at the expense of the broad component that has disappeared by 27°C (Fig. 1 *c*). The shoulders indicate the initiation of fast axial rotation for PSM* at the onset of its transition to the liquid crystalline phase within the mixture with POPE. As shown by the spectrum observed at 52°C that characterizes the lamellar liquid crystalline state (27), a further increase in temperature leads to the resolution of peaks within the spectrum (Fig. 1 *d*). Rapid isomerization

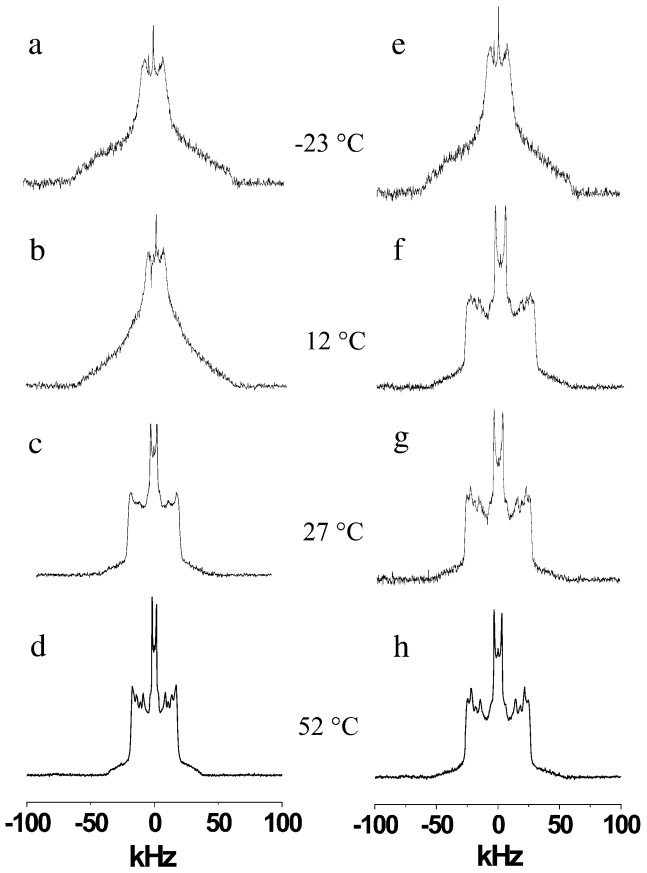

FIGURE 1 ^{2}H-NMR spectra for a 50 wt % aqueous dispersion in 50 mM Tris buffer (pH 7.5) of POPE/PSM*(1:1 mol) (*left panel*) and POPE/PSM*/cholesterol (1:1:1 mol) (*right panel*). Spectra were recorded at −23°C (*a* and *e*), 12°C (*b* and *f*), 27°C (*c* and *g*), and 52°C (*d* and *h*).

about C–C bonds in the [$^2H_{31}$]16:0 chains of PSM* is responsible. A superposition of doublets with similar splitting, corresponding to the plateau region of relatively constant order in the upper part of the chain, produces the well-defined edges at ±19 kHz. Less-ordered methylenes in the lower part of the acyl chain primarily give rise to doublets with dissimilar splitting that appear as the individual peaks within the spectrum, whereas the highly mobile terminal methyl is represented by the central pair of peaks.

Fig. 1 (*right panel*) presents spectra for a 50 wt % aqueous dispersion of POPE/PSM*/cholesterol (1:1:1 mol) in 50 mM Tris (pH 7.5) that illustrate the effect of cholesterol on the phase behavior of PSM* in the OA-containing PE lipid mixture. Although gel-like in form, substantial narrowing due to the presence of cholesterol is apparent in the spectrum at −23°C (Fig. 1 *e*). This spectral narrowing reflects the sterol-induced disruption to the organized packing of acyl chains in the gel state. Even greater perturbation is apparent in the spectrum obtained at 12°C (Fig. 1 *f*). Whereas the spectrum is entirely attributable to gel-phase lipid in the absence of cholesterol (Fig. 1 *b*), the spectrum for PSM* in the mixture with POPE can be assigned completely to the lamellar liquid crystalline phase after the addition of sterol (Fig. 1 *f*). The spectra observed for POPE/PSM*/cholesterol (1:1:1 mol) on heating to 27°C and 52°C (Fig. 1, *g* and *h*) are similarly characteristic of the liquid crystalline state. There is spectral broadening associated with a reduction in *gauche-trans* isomerization along the fluid [$^2H_{31}$]16:0 chain of the sphingolipid by the rigid steroid moiety; this is exemplified by an increase from ±19 to ±26 kHz in the width of the sharp edges that the spectra without (Fig. 1 *d*) and with (Fig. 1 *h*) cholesterol possess at 52°C.

The spectra in Fig. 2 (*left panel*) were recorded for a 50 wt % aqueous dispersion of PDPE/PSM* (1:1 mol) in 50 mM Tris (pH 7.5) (1:1) under the same experimental conditions used with the spectra shown for POPE/PSM* (1:1 mol) in Fig. 1. Differences in the phase behavior of PSM* when mixed with DHA- versus OA-containing PE are revealed by comparing the spectra. The lineshape for PDPE/PSM* (1:1 mol) (Fig. 2 *a*), as for POPE/PSM* (1:1 mol) (Fig. 1 *a*), is gel-like at −23°C. Greater restriction to chain motion is implied for PSM* in the mixture with PDPE by enhanced intensity in the wings of the spectrum. At 12°C, the spectrum for PDPE/PSM* (1:1 mol) (Fig. 2 *b*), unlike POPE/PSM* (1:1 mol) (Fig. 1 *b*), no longer contains the shoulders at ±63 kHz that designate gel phase. Instead, a component of width ±25 kHz representing methylene groups undergoing axial rotation together with a central methyl component comprises the entire spectrum. An additional rise in temperature introduces *gauche-trans* isomerization into the perdeuterated chain of PSM* and leads to the appearance of individual peaks within the methylene component of the spectrum acquired at 27°C (Fig. 2 *c*). These peaks become better resolved on heating, resulting in the observation of the characteristic liquid crystalline powder pattern at 52°C (Fig. 2 *d*). The spectra for PSM* in the mixed membrane with polyunsaturated PDPE at these latter two temperatures resemble those seen with POPE at the equivalent temperatures (Fig. 1, *c* and *d*).

In Fig. 2 (*right panel*), ^{2}H-NMR spectra that were acquired for an aqueous dispersion of PDPE/PSM*/cholesterol (1:1:1 mol) in 50 mM Tris buffer (pH 7.5) demonstrate how adding cholesterol affects the phase behavior of PSM* in the DHA-containing PE mixed membrane. They are qualitatively similar to the spectra seen for POPE/PSM*/cholesterol (1:1:1 mol) (Fig. 1, *right panel*). As in the OA-containing PE mixture, the response to sterol consists of a disordering and ordering of gel-state and liquid crystalline–state PSM*, respectively. Compared to the spectrum for PDPE/PSM* at −23°C (Fig. 2 *a*) that is typical of solely gel phase, a spectral component with shoulders at ±25 kHz, indicating the onset of fast axial rotation for the perdeuterated [$^2H_{31}$]16:0 chain of PSM*, is apparent on the broad gel-like background when cholesterol is present (Fig. 2 *e*). The spectrum becomes completely liquid crystalline–like on heating to 12°C (Fig. 2 *f*), displaying the peaks within the methylene envelope that signify rapid isomerization. Such peaks are not discernible at the corresponding temperature in the spectrum obtained in

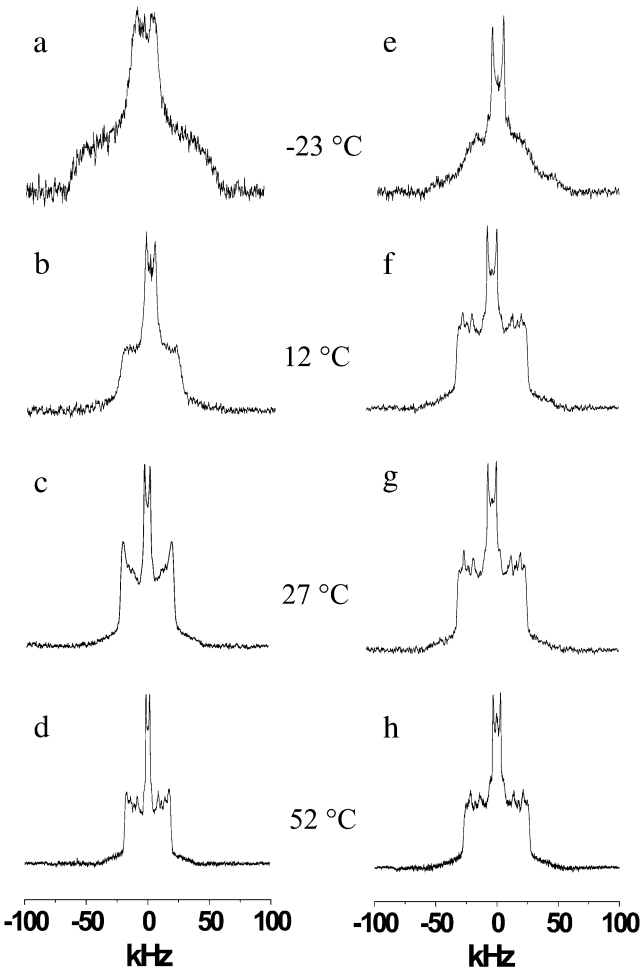

FIGURE 2 ^{2}H-NMR spectra for a 50 wt % aqueous dispersion in 50 mM Tris buffer (pH 7.5) of PDPE/PSM* (1:1 mol) (*left panel*) and PDPE/PSM*/cholesterol (1:1:1 mol) (*right panel*). Spectra were recorded at -23°C (*a* and *e*), 12°C (*b* and *f*), 27°C (*c* and *g*), and 52°C (*d* and *h*).

the absence of sterol (Fig. 2 *b*) and, as illustrated by the spectra at 27°C (Fig. 2 *c*) and 52°C (Fig. 2 *d*), do not appear and subsequently grow in resolution until a higher temperature is reached. In contrast, the spectrum for PDPE/PSM*/cholesterol (1:1:1 mol) changes little other than modestly narrowing over the same temperature interval (Fig. 2, *g* and *h*). The differential in spectral width (±25 kHz vs. ±18 kHz) with (Fig. 2 *h*) and without (Fig. 2 *d*) cholesterol at 52°C is symptomatic of the sterol-induced increase in order for liquid crystalline PSM* in PDPE/PSM* (1:1 mol).

The spectra shown in Figs. 1 and 2 are representative of data obtained in each case over a temperature range that extends from −30°C to 50°C. They illustrate the sensitivity of spectral lineshape to membrane phase. To quantify the shape of all of the spectra, and thereby monitor phase behavior, first moments M_1 were calculated according to Eq. 1; they are plotted against temperature in Fig. 3 for POPE/PSM* (1:1 mol) and for PDPE/PSM* (1:1 mol) in the absence and presence of cholesterol (1:1:1 mol). Slowly varying moments of magnitude $M_1 > 10\times10^4$ s^{-1} (signifying gel phase) and $< 8\times10^4$ s^{-1} (signifying liquid crystalline phase) were measured for POPE/PSM* (1:1 mol) at temperatures <19°C and >24°C, respectively (Fig. 3 *a*). The sharp drop in the value of M_1 that accompanies the transition between states is ~5°C in width and centered at 22.5°C. No discontinuity in the variation of M_1 with temperature remains for PSM* in the OA-containing PE mixture after the addition of cholesterol (Fig. 3 *a*). A broadening of the phase transition to near elimination is indicated by M_1 values that gradually decrease from $10.5 - 8.7\times10^4$ s^{-1} over the entire −30°C–50°C span of temperature studied.

The variation with temperature of the first moments M_1 plotted for PDPE/PSM* (1:1 mol) (Fig. 3 *b*) takes the same form as that observed for POPE/PSM* (1:1 mol) (Fig. 3 *a*). There is an abrupt reduction in the M_1 value centered at 13.7°C and ~4°C in width that is indicative of a precipitous increase in molecular motion. The moments otherwise vary slowly from 13.4×10^4 s^{-1} at −32°C to 10.4×10^4 s^{-1} at 12°C and from 8.2×10^4 s^{-1} at 15°C to 6.2×10^4 s^{-1} at 52°C. It should be noted that, in the region where the dramatic change occurs most markedly (at 12°C), the moments depend on the delay time t between the two 90° pulses in the quadrupolar echo sequence. The values plotted there were obtained by extrapolation to zero delay of M_1 measured as a function of t. We attribute this behavior to the presence of (intermediate) exchange of PSM* between motionally distinct environments in the PDPE/PSM* mixture on a timescale comparable to the delay between pulses. As with POPE/PSM* (Fig. 3 *a*), the moments presented in Fig. 3 *b* for PSM* in the DHA-containing mixed membrane no longer exhibit a discontinuity on the addition of 1:1:1 mol cholesterol. They slowly fall from 10.3×10^4 s^{-1} at −32°C to 8.2×10^{-4}s^{-1} at 52°C. The small range of the M_1 values is consistent with a sterol-associated smearing out of changes in molecular organization with temperature.

DSC

DSC cooling scans for 0.5 wt % aqueous dispersions of POPE/PSM (1:1 mol) (Fig. 3 *c*) and PDPE/PSM (1:1 mol) (Fig. 3 *d*) in 10 mM phosphate buffer (pH 7.4) are included in Fig. 3 for purposes of comparison. The scan for POPE/PSM (1:1 mol) consists of an endotherm that peaks at 25.8°C and is 2.7°C in width at half height (Fig. 3 *c*). It closely resembles the scan recorded using egg SM instead of PSM in our earlier work (17); on the basis of this similarity, the broad endotherm is interpreted as a superposition of two transitions ascribed to POPE-rich/SM-poor and POPE-poor/SM-rich regions that possess very similar transition temperatures. Consistent with this interpretation, the mid-point in the discontinuity of the spectral moments measured in this study for the melting of PSM* in POPE/PSM* (1:1 mol) at 22.5°C (Fig. 3 *a*) is close to that measured previously for POPE* in POPE*/egg SM (1:1 mol) at ~23°C (17). The temperature for the peak of the

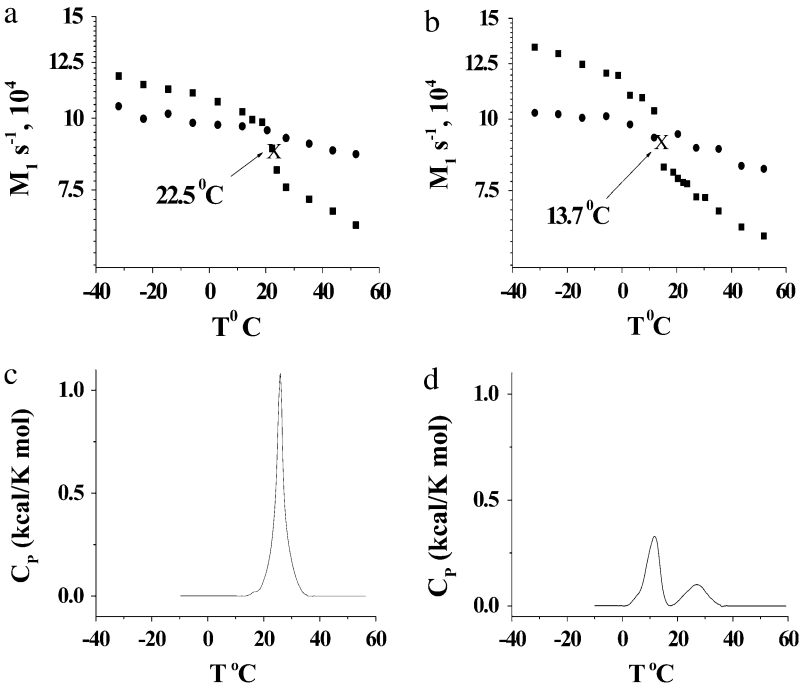

FIGURE 3 Variation of the first moment M_1 as a function of temperature for (*a*) POPE/PSM* (1:1 mol) in the absence (*solid squares*) and presence (*solid circles*) of cholesterol (1:1:1 mol), and (*b*) POPE/PSM* (1:1 mol) in the absence (*solid squares*) and presence (*solid circles*) of cholesterol (1:1:1 mol). M_1 is plotted logarithmically for clarity and the ''X'' designates the midpoint of the sharp drop in moment observed when the sterol is absent. DSC cooling scans for (*c*) POPE/PSM (1:1 mol) and (*d*) PDPE/PSM (1:1 mol). The scans are inverted so that transitions appear as positive peaks.

composite endotherm lies slightly above the temperatures identified from NMR. A lowering by 3°C–4°C of the transition temperature due to perdeuteration (30) is likely responsible for the difference. No endotherm is observed on addition of cholesterol at 1:1:1 mol concentration (data not shown), in agreement with the behavior previously reported for POPE/egg SM/cholesterol (1:1:1 mol) (17).

The cooling scan for PDPE/PSM (1:1 mol) shown in Fig. 3 *d*, in contrast to POPE/PSM (1:1 mol) (Fig. 3 *c*), displays two separate endotherms, as we previously observed with PDPE/egg SM (1:1 mol) (17). The peak temperature of the lower transition assigned to a PDPE-rich/PSM-poor phase is 11.6°C, whereas that of the higher transition assigned to a PDPE-poor/PSM-rich phase is 26.8°C. The temperature of the former transition is near that of an abrupt drop in first moment recorded at ~7°C for PDPE* in PDPE*/egg SM (1:1 mol) in our earlier work (17). The latter transition, however, is much higher in temperature than the precipitous drop centered at 13.7°C revealed in this study by spectral moments for PSM* in PDPE/PSM* (1:1 mol) (Fig. 3 *b*). This divergence, which is too great to be explained by isotopic substitution, is due to the inherently different nature of the two types of measurement. Whereas the transition detected by DSC directly represents the excess specific heat absorbed when lipid acyl chains melt, other molecular motions can lead to the narrowing of NMR spectra reflected in a reduction in moment. This issue will be discussed later. Addition of cholesterol in 1:1:1 mol eliminates both endotherms (data not shown), as was observed in a similar manner when the same concentration of cholesterol was added to PDPE/egg SM (1:1 mol) (17).

Acyl chain order

The liquid crystalline phase is representative of the biological state of lipid molecules. In this phase, during which rapid reorientation of lipid molecules results in spectra symptomatic of axially symmetry, the first moment M_1 calculated from ^{2}H-NMR spectra for perdeuterated lipid chains is related to the $\overline{S}_{CD}$ for the entire chain via Eq. 2. Table 1 lists the $\overline{S}_{CD}$ values obtained at 35°C for POPE/PSM* (1:1 mol), POPE/PSM*/cholesterol (1:1:1 mol), PDPE/PSM* (1:1 mol), and PDPE/[$^2H_{31}$]PSM*/cholesterol (1:1:1 mol). Inspection reveals that, as expected, cholesterol restricts the molecular motion of PSM* in both POPE/PSM* and PDPE/PSM*. In the former, mixture order increases by $\Delta\bar{S}_{CD} = 0.059$ from $\bar{S}_{CD} = 0.237$ to 0.296, whereas in the latter mixture, order increases by $\Delta\bar{S}_{CD} = 0.064$ from $\bar{S}_{CD} = 0.227$ to 0.291.

The relatively modest distinction between the response of the molecular organization of SM to the addition of sterol in the two systems contrasts with the markedly different increase in order revealed for the PE component by $\bar{S}_{CD}$ values for POPE*/egg SM (1:1 mol) and PDPE*/egg SM (1:1 mol) (4), which also are included in Table 1. The data demonstrate that, although the [$^2H_{31}$]16:0 *sn*-1 chain of POPE* ($\bar{S}_{CD} = 0.167$) in POPE*/egg SM (1:1 mol) and PDPE* ($\bar{S}_{CD} = 0.165$) in PDPE*/egg SM (1:1 mol) possesses almost identical order, there is an appreciable differential in the effect of cholesterol (1:1:1 mol). Whereas $\Delta\bar{S}_{CD} = 0.099$ characterizes the elevation in order of the OA-containing PE owing to the sterol, the corresponding change of $\Delta\bar{S}_{CD} = 0.043$ for the DHA-containing PE is substantially less.

TABLE 1 Average order parameters $\bar{S}_{CD}$ derived from ^{2}H-NMR spectra for POPE/PSM* (1:1 mol) and PDPE/PSM* (1:1 mol) in the absence and presence of cholesterol (1:1:1 mol) at 35°C

	No cholesterol	With cholesterol	
Membrane composition	$\bar{S}_{CD}$		$\Delta\bar{S}_{CD}$
POPE/PSM*	0.237	0.296	0.059
POPE*/egg SM†	0.167	0.266	0.099
PDPE/PSM*	0.227	0.291	0.064
PDPE*/egg SM†	0.165	0.208	0.043

Corresponding values for POPE*/egg SM (1:1 mol) and PDPE*/egg SM (1:1 mol) are included for comparison.
†Values taken from Wassall et al. (4)

To elaborate on the distribution of order along the perdeuterated [$^2H_{31}$]16:0 amide chain of PSM* in the mixed membranes, the NMR signals were fast Fourier transform depaked (26). The result of the application of this algorithm to POPE/PSM* (1:1 mol) (Fig. 4, *a* and *b*) and PDPE/PSM* (1:1 mol) (Fig. 4, *c* and *d*) in the absence and presence of cholesterol (1:1:1 mol), respectively, at 44°C is shown in Fig. 4. The depaked spectra consist of an outermost composite doublet, representing comparably ordered methylene groups in the upper part of the chain, and a series of four doublets with smaller splittings, predominantly corresponding to increasingly less ordered methylene groups and terminal methyl group in the lower portion of the chain. The vast enhancement in resolution achieved relative to the powder pattern facilitates the generation of a profile of order parameter with the aid of Eq. 3. The procedure, apart from the C2 position, consists of assigning equal intensity to each methylene group and assuming a continuous decrease of order toward the terminal methyl (29). Constraints imposed on the initial orientation of the amide chain of SM (30), like with the *sn*-2 chain of phospholipids (33), render the C2 position an exception to the assumption that order varies monotonically. The two motionally inequivalent deuterons at this position possess different splittings that were assigned as indicated in Fig. 4 on the basis of intensity and comparison with work on selectively deuterated PSM (30).

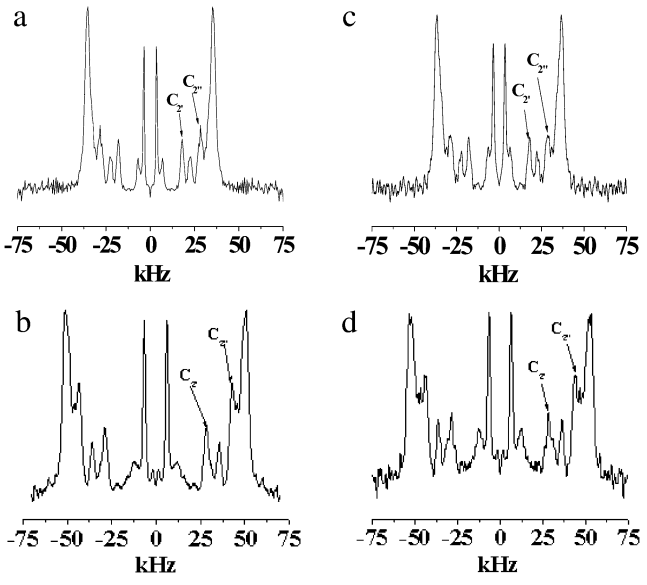

FIGURE 4 Fast Fourier transform depaked spectra for POPE/PSM* (1:1 mol) in the absence (*a*) and presence (*b*) of cholesterol (1:1:1 mol), and for PDPE/PSM* (1:1 mol) in the absence (*c*) and presence (*d*) of cholesterol (1:1:1 mol) at 43°C. The arrows specify assignment of the C2 position.

The order parameter profiles created from the depaked spectra in Fig. 4 are shown in Fig. 5. It is apparent that the same general form is observed in each case. There is a plateau region of approximately constant order in the upper portion of the chain (C3–C12) followed by progressively less order toward the bottom of the chain (C13–C16). This shape is characteristic of phospholipids (34) and sphingolipids (30) in the lamellar liquid crystalline phase. It is retained when cholesterol is added to POPE/PSM* (1:1 mol) (Fig. 5 *a*) and PDPE/PSM* (1:1 mol) (Fig. 5 *b*), with the increase in $\bar{S}_{CD}$ calculated from M_1 (Table 1) manifest as higher S_{CD} values throughout the chain.

DISCUSSION

A diverse collection of health benefits accrues from the dietary consumption of PUFA, the most notable of which is DHA (35). We have hypothesized that changes in membrane architecture in response to elevated levels of DHA-containing phospholipids are, in part, responsible for these benefits (3–5). Our hypothesis juxtaposes the tremendously high disorder of PUFA chains, for which close proximity to cholesterol is incompatible, with the highly ordered conformation adopted by the mostly saturated chains of sphingolipids in sterol-enriched lipid rafts. Due to the differential in affinity, cholesterol further segregates into lipid rafts away from PUFA-rich domains that form when polyunsaturated phospholipids substitute for bulk less unsaturated phospholipids in the plasma membrane. It is the concomitant movement of signaling proteins into and out of rafts and the resultant modulation of cell signaling to which the relief of disease states by DHA is ascribed.

Mixtures of PDPE with SM and cholesterol are a model membrane system that we have developed to characterize the sorting of lipids into PUFA-rich/sterol-poor (nonraft) and SM-rich/sterol-rich (raft) domains. Early DSC work on ternary lipid/lipid/cholesterol mixtures indicated that cholesterol associates with PE less strongly than with PC and SM (36). This finding, as well as a diminished affinity for polyunsaturated phospholipids, was confirmed by an assay with cyclodextrin of partition coefficients for cholesterol in unilamellar vesicles (37). Unequivocal substantiation of aversion for the sterol is provided by the substantially lower solubility measured for cholesterol in PDPE (32 mol %) compared to the equivalent DHA-containing PC and PE or PC that does not possess a PUFA chain (≥50 mol %) (21). A greater propensity for PDPE* than for monounsaturated

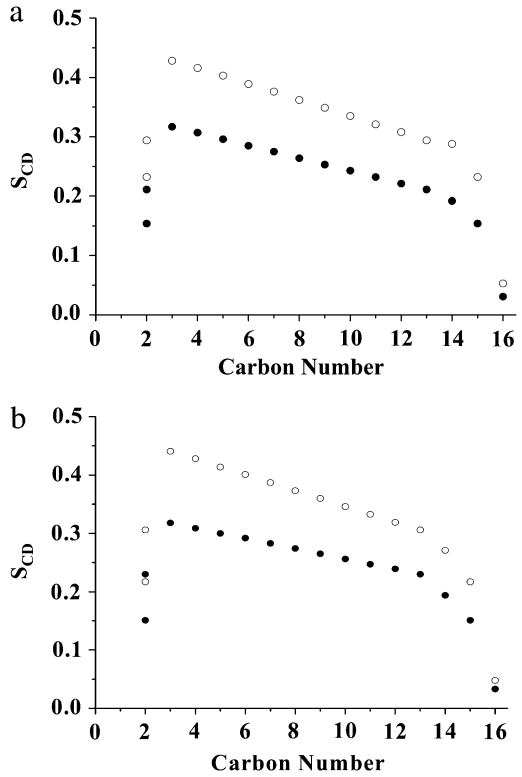

FIGURE 5 Order parameter profiles generated from depaked spectra for (a) POPE/PSM* (1:1 mol) in absence (*solid circles*) and presence (*open circles*) of cholesterol (1:1:1 mol), and for (*b*) PDPE/PSM* (1:1 mol) in absence (*solid circles*) and presence (*open circles*) of cholesterol (1:1:1 mol) at 43°C.

POPE* to separate into nonraft domains when mixed in 1:1:1 mol ratio with SM and cholesterol was inferred, in particular, on the basis of ^{2}H-NMR data gathered in an earlier study (17). In this report, we investigate the same system from a different perspective. We compare ^{2}H-NMR spectra for PSM* in 1:1:1 mol combination with PDPE or POPE and cholesterol, complemented by DSC, to elucidate molecular organization of the SM-component in the mixed model membrane system.

Segregation into SM-rich and PE-rich nanosized domains

The DSC results presented in Fig. 3 reveal two separate endotherms in the scan for PDPE/PSM (1:1 mol) with peaks at 11.6°C and 26.8°C (Fig. 3 *d*), indicating that the two lipids mix inhomogeneously. Because the transition temperatures do not match those for single-component PDPE and PSM membranes for which $T_m = 2.2$°C (22) and 41°C (32), respectively, the demixing is considered incomplete. The lower temperature endotherm that is elevated 9°C with respect to pure PDPE is assigned to a PE-rich/SM-poor phase, whereas the higher temperature endotherm that is depressed 14°C with respect to pure PSM is assigned to a PE-poor/SM-rich phase. This assignment corresponds to the one made in our previous DSC work on PDPE/egg SM (1:1 mol) (17). Although, in contrast, only one endotherm with a peak at 25.8°C is observed for POPE/PSM (1:1 mol) (Fig. 3 *c*), inhomogeneous mixing into PE-rich/SM-poor and PE-poor/SM-rich domains also is concluded in mixtures with the monounsaturated PE. Thermograms recorded for different relative concentrations of lipid in the highly similar POPE/egg SM system exhibit two individual transitions that overlap at 1:1 mol ratio (17). We attribute this overlap to the higher transition temperature of pure POPE ($T_m = 25.5$°C) (22) compared to PDPE. The result is a smaller differential in temperature between the endotherms ascribed to PE-rich and SM-rich phases for mixtures of SM with OA- compared with DHA-containing PE.

Table 1 provides further insight into the segregation of PE and SM into domains. Average order parameters $\bar{S}_{CD}$ derived from ^{2}H-NMR spectra at 35°C are shown for PSM* mixed at 1:1 mol with PDPE or POPE and for PDPE* or POPE* mixed at 1:1 mol with egg SM, both in the absence and presence of cholesterol at 1:1:1 mol concentration. Higher $\bar{S}_{CD}$ values for SM than for PE are exhibited in each mixture, exemplified by $\bar{S}_{CD} = 0.291$ for PSM* in PDPE/PSM*/cholesterol versus $\bar{S}_{CD} = 0.208$ for PDPE* in PDPE*/egg SM/cholesterol. The implied motional inequivalence is consistent with our interpretation of the DSC data for PE/SM mixtures in terms of separation into domains. Moreover, the distinction in $\bar{S}_{CD}$ value that remains with PE/SM/cholesterol (1:1:1 mol) mixtures for which the addition of cholesterol broadens endotherms beyond DSC detection demonstrates that the separation of PE and SM into domains persists in the presence of the sterol.

Despite incomplete demixing of PE and SM, a superposition of individual spectral components from PSM* in SM-rich/PE-poor and SM-poor/PE-rich domains is not discernible in the spectra for the various mixtures with PE and cholesterol (Figs. 1 and 2). The same assessment applies to our previously published spectra for PDPE* and POPE* in corresponding mixtures with egg SM and sterol (17). The implication is a fast exchange of lipids in and out of domains occurring at a rate greater than the differential in quadrupolar splitting between the environments when the mixed membrane is entirely liquid crystalline. The resultant spectrum is a time average in which the lipid contributes intensity that is weighted according to its population in each domain. Assuming that the spectra for deuterated SM and PE are approximately representative of SM- and PE-rich environments, respectively, an upper estimate to the size of domains then may be deduced with the aid of the average order parameters in Table 1. The calculation employs 0.08 for the difference in $\bar{S}_{CD}$ value between domains, referring to PDPE/PSM*/cholesterol versus PDPE*/egg SM/cholesterol for which the divergence is greatest and would yield the most generally applicable estimate for domain size. This difference in $\bar{S}_{CD}$ equates to a difference of $\Delta\nu = 10$ kHz in average

splitting, according to which the lifetime for the residency of lipid molecules in a domain must be less than $\tau = (2\pi\Delta\nu)^{-1} = 2x10^{-5}$ s. The exchange of lipids between domains is presumed to be mediated by lateral diffusion with $D \sim 5 \times 10^{-12}$ m^{2}s^{-1} (38), so that an upper limit of <20 nm is placed on the radius of domains via the root mean-square displacement $r = (4D\tau)^{1/2}$ associated with the lifetime. Such domains, if treated as circular, would contain <1800 lipid molecules of mean cross-sectional area 70 Å^2 (22) in each leaflet. They could certainly accommodate estimates of 52 and 75 for the number of PDPE and PSM molecules, respectively, undergoing a cooperative transition evaluated on the basis of the ratio of van 't Hoff and calorimetric enthalpies (39) from the transitions ascribed to PE-and SM-rich domains in the DSC cooling scan for PDPE/PSM (Fig. 3 *d*).

The size obtained in this study for domains falls at the low end of the 10–200 nm range reported for sphingolipid- and sterol-enriched membrane rafts (13) and is comparable with estimates for PUFA-rich patches in model membranes (6,40). 1-stearoyl-2-docosahexaenoylphosphatidylcholine (SDPC)/cholesterol clusters <25 nm in radius were identified in PC/PE/PS (4:4:1 mol) membranes on the basis of an appraisal of ^{2}H-NMR data for perdeuterated analogs of each phospholipid (6). ^{2}H-NMR powder pattern spectra recorded for 1,2-diarachidonylphosphatidylcholine (DAPC)/1-stearoyl-2-arachidonylphosphatidylcholine (SAPC)/[3α-^{2}H$_1$]cholesterol (1:1:2 mol) were analyzed in terms of the partitioning of DAPC and SAPC into regions that extend for <16 nm, the sterol preferentially sequestering away from the dipolyunsaturated phospholipid (40). An assumption of fast exchange of lipid back-and-forth between domains, as in this work, is central to spectral interpretation in these previous studies.

Exchange of SM among SM-rich/PE-poor and SM-poor/PE-rich domains offers a possible explanation for the apparent discrepancy in transition temperature identified by ^{2}H-NMR spectral moments (Fig. 3 *b*) and by the DSC cooling scan (Fig. 3 *d*) for mixtures with DHA-containing PE. The abrupt drop in value of M_1 for PSM* in PDPE/PSM* centers on 13.7°C (Fig. 3 *b*). This temperature is 13°C lower than that of the endotherm at 26.8°C assigned to the SM-rich phase, but only just above that of the endotherm at 11.6°C assigned to the PE-rich phase in DSC cooling scans for PDPE/PSM (Fig. 3 *d*). We attribute the reduction in M_1 to the movement of PSM* between gel-like SM-rich/PE-poor and liquid crystalline–like SM-poor/PE-rich regions. The dependence on delay between pulses in the quadrupolar echo sequence used to acquire data for M_1 values in the vicinity of the discontinuity in their temperature variation implies an exchange rate that is intermediate in rate on a timescale comparable to the delay time. Slower lateral diffusion is presumably responsible. Only at higher temperatures that are above those ascribed to the transition for the SM-rich/PE-poor phase by DSC scans do the ^{2}H-NMR spectra for PSM* in PDPE/PSM* attain the resolution characteristic of the liquid crystalline state (Fig. 2 *c* and *d*). Exchange of PSM* between gel- and liquid crystalline–like phases does not complicate spectral interpretation for POPE/PSM* because, in contrast, the transitions due to PE-rich/SM-poor and PE-poor/SM-rich phases coincide in temperature for 1:1 mol mixtures with the OA-containing phospholipid (Fig. 3 *c*).

PUFA-cholesterol aversion excludes sterol from DHA-containing PE-rich domains

The impact of cholesterol on the acyl chain order of each component in the mixtures of OA- and DHA-containing PE with SM (1:1:1 mol) is elaborated by the collation of average order parameters $\bar{S}_{CD}$ shown in Table 1. An increase in $\bar{S}_{CD}$ value for all membrane constituents due to sterol is apparent, which is indicative of incorporation into SM-rich and PE-rich domains for both systems. This effect is manifest throughout the acyl chain, as demonstrated by the order parameter profiles shown for PSM* with POPE or PDPE in Fig. 5 and previously reported for POPE* or PDPE* with egg SM (17). The plateau region of slowly varying order in the upper portion of the chain is elevated, and the overall shape of the profile is retained. A significant difference in the pattern that the cholesterol-induced change in average order $\Delta\bar{S}_{CD}$ has undergone exists between the system containing the polyunsaturated phospholipid and the control containing the monounsaturated phospholipid. There is a slightly larger rise in order for PSM* in PDPE/PSM* ($\Delta\bar{S}_{CD} = 0.064$) than in POPE/PSM* ($\Delta\bar{S}_{CD} = 0.059$). The differential, however, is comparable with the uncertainty (± 0.005) that accompanies the reproducibility ($\pm 1\%$) typically encountered with the measurement of first moments. In stark contrast, the $\bar{S}_{CD}$ values provided in Table 1 from our previous work exhibit a substantially smaller increase due to the presence of sterol for PDPE* in PDPE*/egg SM ($\Delta\bar{S}_{CD} = 0.043$) than for POPE* in POPE*/egg SM ($\Delta\bar{S}_{CD} = 0.099$) (4).

To interpret the changes $\Delta\bar{S}_{CD}$ in average order due to cholesterol listed in Table 1 in terms of the degree of localization of the sterol into a domain, it is necessary to appreciate how each lipid individually responds to the presence of cholesterol. The ordering effect of a given concentration of cholesterol on PDPE* and POPE* is comparable, whereas SM (like PC) is more sensitive (41–43). In a previous study, we measured a rise in $\bar{S}_{CD}$ by 0.04 when 50 mol % cholesterol was added to PDPE* (41). Recognizing that the solubility of the sterol in PDPE is ~30 mol % (21), the rise we observed is similar to the increase of 0.05 in $\bar{S}_{CD}$ seen for POPE* with 30 mol % cholesterol (42). Increases of >0.1 in average order due to 30 mol % sterol were exerted on PSM* (K. Beyer, unpublished) and bovine brain SM, as detected with 5 mol % 1,2-dipalmitoylphosphatidylcholine (DPPC) perdeuterated in the *sn*-1 chain as a probe (43). That the increase $\Delta\bar{S}_{CD}$ in average order for PDPE* in PE/SM (1:1 mol) mixtures due to cholesterol (1:1:1 mol) is less than half that for POPE* (Table 1), thus, implies a greater tendency for PDPE* than POPE* to

segregate into PE-rich domains depleted in sterol. The measurements performed on PSM* in this study, however, belie the simple expectation that the opposite trend might apply to the $\Delta\bar{S}_{CD}$values for PSM* in the analogous PE/SM mixtures. Only a slightly greater increase in order (0.064 vs. 0.059) due to cholesterol is evident for PSM* in the PDPE- rather than the POPE-containing mixture, and the resultant order for PSM* in both systems is close (Table 1). We speculate that the effect of the sterol on the order of PSM* is modulated by the presence of PE in the SM-rich domains. Remarkably, the SM-rich, raft-like domains appear almost equally ordered in the PDPE/PSM*/cholesterol and POPE/PSM*/cholesterol membranes.

The net effect of DHA versus OA in the presence of cholesterol is to accentuate the distinction in molecular organization between the environment within SM-rich (more ordered) and PE-rich (less ordered) domains. Although the difference in average order $\bar{S}_{CD}$ between the domains revealed by Table 1 in the POPE/SM/cholesterol mixture is 0.030 and modest, the difference in the PDPE/SM/cholesterol mixture is 0.083 and almost a factor of 3 bigger. These figures, which underestimate the disparity due to fast exchange of lipid molecules between domains, correspond to a differential of 11 and 33% (relative to the mean $\bar{S}_{CD}$ for a mixture), respectively. Further, physical insight into the molecular architecture of the domains is gleaned from $\bar{S}_{CD}$ by invoking the following:

$$\langle L\rangle = l(0.5 + |\bar{S}_{CD}|) \quad (4)$$

to obtain the average length $\langle L\rangle$ of [$^2H_{31}$]16:0 chains in a bilayer, where $l = 19.1$ Å is the length of the chain projected onto the bilayer normal in the all-*trans* configuration (44,45). The thickness of the bilayer in SM-rich and PE-rich domains then may be estimated from the data in Table 1. There are two important assumptions involved: 1), the dominant contribution to the population-weighted average $\bar{S}_{CD}$ values produced by fast exchange between domains comes from the environment in which a lipid is enriched, and 2), $\langle L\rangle$ approximates to the thickness of a monolayer. The calculation yields estimates of 30.4 Å for PSM* and 29.2 Å for POPE* in their 1:1:1 mol mixtures with cholesterol, as opposed to 30.2 Å for PSM* and 27.0 Å for PDPE* in their 1:1:1 mol mixtures with cholesterol. Replacing OA with DHA, thus, increases the divergence in thickness between SM-rich and PE-rich domains from 1.2 to 3.2 Å.

We attribute the difference in response to cholesterol of the DHA- and OA-containing PE mixtures with SM to the mutual aversion that PUFA and sterol possess. A graphic depiction of our explanation is shown in Fig. 6. In the absence of cholesterol, PDPE and SM segregate into nanosized domains that are PE-rich and SM-rich (Fig. 6, *top left*). When cholesterol is added, it preferentially partitions into SM-rich domains and tends to further exclude PDPE into PUFA-rich domains (Fig. 6, *top right*). This partitioning is due to the differential affinity the sterol possesses for PDPE versus SM, not because it has exceeded its solubility in PDPE-rich domains. Exclusion of PUFA-containing phospholipid driven by incompatibility with the highly ordered matrix formed by SM and cholesterol is an alternative mechanism that would produce the same effect, which was recently proposed by Lindblom and coworkers (46) in a study of lipid diffusion in PC/SM/cholesterol mixtures. Accordingly, the polyunsaturated phospholipid has less contact with the sterol and experiences only a modest increase in order. POPE and SM similarly separate into PE-rich and SM-rich domains in a membrane devoid of sterol (Fig. 6, *bottom left*), although

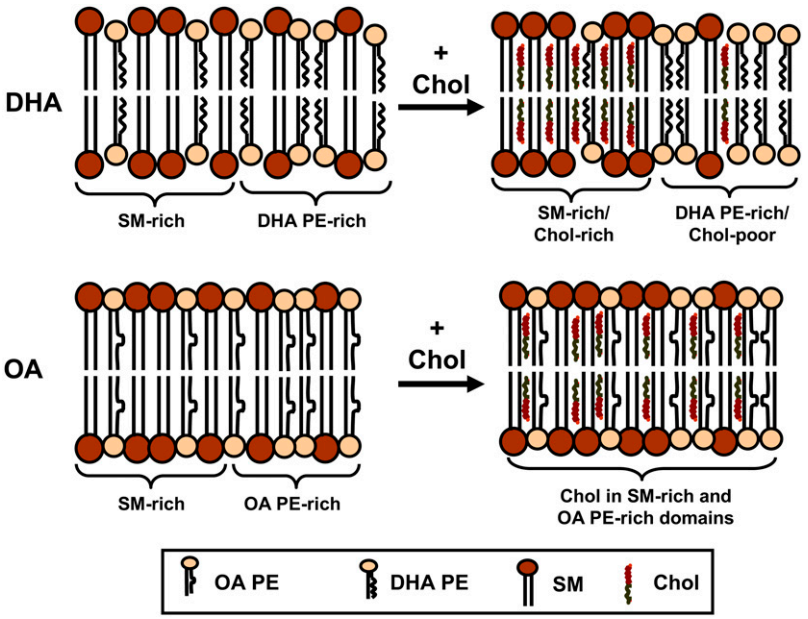

FIGURE 6 A graphic depiction of DHA versus OA-induced lateral segregation of lipid molecules in PE/SM/cholesterol (1:1:1 mol) membranes. PE-rich and SM-rich domains coexist in PDPE/SM (*top left*) and POPE/SM (*bottom left*) membranes in the absence of sterol. On addition of cholesterol to PDPE/SM, the sterol is preferentially taken up into SM-rich domains for which it has high affinity and further displaces DHA for which it has low affinity. The formation of DHA-containing PE-rich/cholesterol-poor nonraft and SM-rich/cholesterol-rich raft domains is the result (*top right*). On addition of cholesterol to POPE/SM, in contrast, the sterol incorporates into OA-containing PE-rich, albeit to a less extent, as well as SM-rich domains (*bottom right*). The tremendous aversion of cholesterol for DHA is not possessed by OA.

probably not to the same extent as with DHA. When cholesterol is introduced, however, the diminished affinity it has for monounsaturated POPE relative to SM is less pronounced than for PDPE. The sterol mixes into OA-containing PE-rich domains as well as into SM-rich domains (Fig. 6, *bottom right*). By virtue of greater proximity, there is then a substantial sterol-associated increase in order for the monounsaturated phospholipid in the mixture. Consistent with this behavior, fast exchange of sterol between two equally populated pools was also inferred from ^{2}H-NMR spectra recorded for a deuterated analog of cholesterol added to 1-plamitoyl-2-oleoylphosphatidylcholine (POPC)/brain SM (1:1:1 mol) (47). Quantitative estimation of the partitioning of cholesterol between domains, an issue complicated by incomplete demixing of SM and PE and their likely redistribution following the introduction of sterol, cannot be made with the mixtures studied in our article.

CONCLUSION

The coexistence of PUFA-rich/cholesterol-poor (nonraft) and SM-rich/cholesterol-rich (raft) domains within plasma membranes has the potential to be the molecular origin, in part, of the multitude of health benefits associated with dietary consumption of fish oils (5). Movement of signaling proteins between these organizationally distinct domains then modulates cellular events via changes in protein conformation. The results of this study establish the lipid-driven formation of such domains. When PDPE substitutes for POPE in PE/SM/cholesterol mixtures, the differential in order and membrane thickness between PE-rich and SM-rich domains becomes approximately 3× greater.

The authors thank K. Beyer for communicating ^{2}H-NMR data before publication.

This work was supported in part by grants from the National Institutes of Health (CA 57212 to W.S. and HL 083187 to R.B.).

REFERENCES

1. Salem, N., Jr., B. Litman, H. Y. Kim, and K. Gawrisch. 2001. Mechanisms of action of docosahexaenoic acid in the nervous system. *Lipids*. 36:945–959.
2. Salem, N., H. Y. Kim, and J. A. Yergey. 1986. Docosahexaenoic Acid: Membrane Function and Metabolism. Academic Press, New York.
3. Stillwell, W., and S. R. Wassall. 2003. Docosahexaenoic acid: membrane properties of a unique fatty acid. *Chem. Phys. Lipids*. 126:1–27.
4. Wassall, S. R., M. R. Brzustowicz, S. R. Shaikh, V. Cherezov, M. Caffrey, and W. Stillwell. 2004. Order from disorder, corralling cholesterol with chaotic lipids. The role of polyunsaturated lipids in membrane raft formation. *Chem. Phys. Lipids*. 132:79–88.
5. Stillwell, W., S. R. Shaikh, M. Zerouga, R. Siddiqui, and S. R. Wassall. 2005. Docosahexaenoic acid affects cell signaling by altering lipid rafts. *Reprod. Nutr. Dev*. 45:559–579.
6. Huster, D., K. Arnold, and K. Gawrisch. 1998. Influence of docosahexaenoic acid and cholesterol on lateral lipid organization in phospholipid mixtures. *Biochemistry*. 37:17299–17308.
7. Mitchell, D. C., and B. J. Litman. 1998. Effect of cholesterol on molecular order and dynamics in highly polyunsaturated phospholipid bilayers. *Biophys. J*. 75:896–908.
8. Singer, S. J., and G. L. Nicolson. 1972. The fluid mosaic model of the structure of cell membranes. *Science*. 175:720–731.
9. Jacobson, K., E. D. Sheets, and R. Simson. 1995. Revisiting the fluid mosaic model of membranes. *Science*. 268:1441–1442.
10. Simons, K., and E. Ikonen. 1997. Functional rafts in cell membranes. *Nature*. 387:569–572.
11. Edidin, M. 2003. The state of lipid rafts: from model membranes to cells. *Annu. Rev. Biophys. Biomol. Struct*. 32:257–283.
12. Brown, D. A., and E. London. 2000. Structure and function of sphingolipid- and cholesterol-rich membrane rafts. *J. Biol. Chem*. 275:17221–17224.
13. Pike, L. J. 2006. Rafts defined: a report on the Keystone symposium on lipid rafts and cell function. *J. Lipid Res*. 17:1597–1598.
14. Simons, K., and R. Ehehalt. 2002. Cholesterol, lipid rafts, and disease. *J. Clin. Invest*. 110:597–603.
15. Simons, K., and W. L. Vaz. 2004. Model systems, lipid rafts, and cell membranes. *Annu. Rev. Biophys. Biomol. Struct*. 33:269–295.
16. Bittman, R., C. R. Kasireddy, P. Mattjus, and J. P. Slotte. 1994. Interaction of cholesterol with sphingomyelin monolayers and vesicles. *Biochemistry*. 33:11776–11781.
17. Shaikh, S. R., A. C. Dumaual, A. Castillo, D. LoCascio, R. A. Siddiqui, W. Stillwell, and S. R. Wassall. 2004. Oleic and docosahexaenoic acid differentially phase separate from lipid raft molecules: a comparative NMR, DSC, AFM, and detergent extraction study. *Biophys. J*. 87:1752–1766.
18. Gennis, R. B. 1989. Biomembranes. Springer-Verlag, New York.
19. Zerouga, M., W. Stillwell, J. Stone, A. Powner, and L. J. Jenski. 1996. Phospholipid class as a determinant in docosahexaenoic acid's effect on tumor cell viability. *Anticancer Res*. 16:2863–2868.
20. Anderson, R. E., and L. Sperling. 1971. Lipids of ocular tissues. VII. Positional distribution of the fatty acids in the phospholipids of bovine retina rod outer segments. *Arch. Biochem. Biophys*. 144:673–677.
21. Shaikh, S. R., V. Cherezov, M. Caffrey, S. P. Soni, D. LoCascio, W. Stillwell, and S. R. Wassall. 2006. Molecular organization of cholesterol in unsaturated phosphatidylethanolamines: x-ray diffraction and solid state ^{2}H NMR reveal differences with phosphatidylcholines. *J. Am. Chem. Soc*. 126:5375–5383.
22. Shaikh, S. R., M. R. Brzustowicz, N. Gustafson, W. Stillwell, and S. R. Wassall. 2002. Monousaturated PE does not phase separate from the lipid raft molecules sphingomyelin and cholesterol: role for polyunsaturation? *Biochemistry*. 41:10593–10602.
23. Barenholz, Y. 1984. Sphingomyelin-lecithin balance in membrane: composition, structure, and function relationships. *In* Physiology of Membrane Fluidity, Vol. 1. M. Shinitsky, editor, CRC Press, Boca Raton, FL. 131–174.
24. Bittman, R., and C. A. Verbicky. 2000. Methanolysis of sphingomyelin. Toward an epimerization-free methodology for the preparation of D-erythro-sphingosylphosphocholine. *J. Lipid Res*. 41:2089–2093.
25. Nyholm, T., M. Nylund, A. Soderholm, and J. P. Slotte. 2003. Properties of palmitoyl phosphatidylcholine, sphingomyelin, and dihydrosphingomyelin bilayer membranes as reported by different fluorescent reporter molecules. *Biophys. J*. 84:987–997.
26. McCabe, M. A., and S. R. Wassall. 1997. Rapid deconvolution of NMR powder spectra by weighted fast Fourier transformation. *Solid State Nucl. Magn. Reson*. 10:53–61.
27. Davis, J. H., K. R. Jeffery, M. Bloom, M. I. Valic, and T. P. Higgs. 1976. Quadrupolar echo deuteron magnetic resonance spectroscopy in ordered hydrocarbon chains. *Chem. Phys. Lett*. 42:390–394.
28. Davis, J. H. 1983. The description of membrane lipid conformation, order and dynamics by ^{2}H-NMR. *Biochim. Biophys. Acta*. 737:117–171.
29. Lafleur, M., B. Fine, E. Sternin, P. R. Cullis, and M. Bloom. 1989. Smoothed orientational order profile of lipid bilayers by ^{2}H-nuclear magnetic resonance. *Biophys. J*. 56:1037–1041.

30. Mehnert, T., K. Jacob, R. Bittman, and K. Beyer. 2006. Structure and lipid interaction of *N*-palmitoylsphingomyelin in bilayer membranes as revealed by ^{2}H-NMR spectroscopy. *Biophys. J.* 90:939–946.

31. Shaikh, S. R., A. C. Dumaual, L. J. Jenski, and W. Stillwell. 2001. Lipid phase separation in phospholipid bilayers and monolayers modeling the plasma membrane. *Biochim. Biophys. Acta.* 1512:317–328.

32. Maulik, P. R., and G. G. Shipley. 1996. *N*-palmitoyl sphingomyelin bilayers: structure and interaction with cholesterol. *Biochemistry.* 35: 8025–8034.

33. Engel, A. K., and D. Cowburn. 1981. The origin of multiple quadrupole couplings in the deuterium NMR spectra of the 2 chain of 1,2 dipalmitoyl-*sn*-glycero-3-phosphorylcholine. *FEBS Lett.* 126:169–171.

34. Seelig, J. 1977. Deuterium magnetic resonance: theory and application to lipid membranes. *Q. Rev. Biophys.* 10:353–418.

35. Stillwell, W., S. R. Shaikh, D. LoCascio, R. A. Siddiqui, J. Seo, R. S. Chapkin, and S. R. Wassall. 2006. Docosahexaenoic acid. An influential membrane-altering omega-3 fatty acid. *In* Frontiers in Nutrition Research. J. D. Huang, editor. Nova Science Publishers, Hauppauge, NY. 249–271.

36. van Dijk, P. W. 1979. Negatively charged phospholipids and their position in the cholesterol affinity sequence. *Biochim. Biophys. Acta.* 555:80–101.

37. Niu, S. L., and B. J. Litman. 2002. Determination of membrane cholesterol partition coefficient using a lipid vesicle-cyclodextrin binary system: effect of phospholipid acyl chain unsaturation and headgroup composition. *Biophys. J.* 83:3408–3415.

38. Filippov, A., G. Orädd, and G. Lindblom. 2006. Sphingomyelin structure influences the lateral diffusion and raft formation in lipid bilayers. *Biophys. J.* 90:2086–2092.

39. Sturtevant, J. M. 1974. Phase transitions of phospholipids. *In* Quantum Statistical Mechanics in the Natural Sciences. B. Kursunogla, S. Mintz, and S. Widmayer, editors. Plenum Press, New York. 63–83.

40. Brzustowicz, M. R., V. Cherezov, M. Caffrey, W. Stillwell, and S. R. Wassall. 2002. Molecular organization of cholesterol in polyunsaturated membranes: microdomain formation. *Biophys. J.* 82:285–298.

41. Shaikh, S. R., V. Cherezov, M. Caffrey, W. Stillwell, and S. R. Wassall. 2003. Interaction of cholesterol with a docosahexaenoic acid-containing phosphatidylethanolamine: trigger for microdomain/raft formation? *Biochemistry.* 42:12028–12037.

42. Paré, C., and M. Lafleur. 1998. Polymorphism of POPE/cholesterol system: a ^{2}H nuclear magnetic resonance and infrared spectroscopic investigation. *Biophys. J.* 74:899–909.

43. Guo, W., V. Kurze, T. Huber, N. H. Afdhak, K. Beyer, and J. A. Hamilton. 2002. A solid-state NMR study of phospholipid-cholesterol interactions: sphingomyelin-cholesterol binary sysetms. *Biophys. J.* 83: 1465–1478.

44. Holte, L. L., S. A. Peter, T. M. Sinnwell, and K. Gawrisch. 1995. ^{2}H nuclear magnetic resonance order parameter profiles suggest a change of molecular shape for phosphatidylcholines containing a polyunsaturated acyl chain. *Biophys. J.* 63:2396–2403.

45. Nagle, J. F. 1993. Area/lipid of bilayers from NMR. *Biophys. J.* 64: 1476–1481.

46. Filippov, A., G. Orädd, and G. Lindblom. 2007. Domain formation in model membranes studied by pulsed-field gradient-NMR: the role of lipid polyunsaturation. *Biophys. J.* 93:3182–3190.

47. Aussenac, F., M. Tavares, and E. J. Dufourc. 2003. Cholesterol dynamics in membranes of raft composition: a molecular point of view from ^{2}H and ^{31}P solid-state NMR. *Biochemistry.* 42:1383–1390.